An experimental model of wind-induced rafting of pancake ice floating on waves

A. Dolatshah[1,2], L. G. Bennetts[3], M. H.. Meylan[4], J. P. Monty[5], A. Toffoli[2]

[1]Faculty of Science, Engineering and Technology, Swinburne University of Technology, Melbourne, VIC 3122, Australia.

[2]Department of Infrastructure Engineering, University of Melbourne, Parkville, VIC 3010, Australia.

[3]School of Mathematical Sciences, University of Adelaide, Adelaide, SA 5005, Australia.

[4]School of Mathematical and Physical Sciences, University of Newcastle, Callaghan, NSW 2308, Australia.

[5]Department of Mechanical Engineering, University of Melbourne, Parkville, VIC 3010, Australia.

1   Introduction

The first stage in sea ice development is the formation of individual ice crystals on the ocean surface. Under rough conditions with the influence of wave, the crystals, frazil, coagulate and consolidate into small circular discs called pancake ice. The pancakes are up to a few meters in diameter and up to 0.4 m thick. In the Antarctic, 50% of the sea ice area is made up by pancake ice floes with diameters $2.3 - 4\,m$ while floes distribution shows two distinct slopes on either sides of this range. Welding of pancakes forms large floes (Alberello et al. , 2018). During the consolidation process, rafting of these pancakes could play a significant role in defining the ice cover thickness, much more than thermodynamic growth (Dai et al. , 2004).

Indirect observations made after wave-ice interactions have revealed clear evidence of rafting process. Ice samples taken in the Weddell Sea (Ackley and Shen , 1996) and Sea of Okhotsk (Toyota , 1998) showed layered structures in the thin sections. Typically, the number of layers varied from two up to seven. A better understanding of the mechanical thickening on top of thermodynamic thickening of a pancake ice field is critical to accurate formulation of spatial and temporal change of ice thickness. Here mechanical thickening is defined as the redistribution of existing ice volume. Martin and Kauffman (1981) and Bauer and Martin (1983) studied frazil ice cover thickness to wave parameters. They suggested that the ice growth rate in a wave field is an order of magnitude greater than the one-dimensional thermal growth model (Anderson , 1961). Hibler and Ackley (1983) showed that thermodynamic ice models underestimate the Weddell Sea ice area evolution in the ice formation season. The dynamics near the ice edge is extremely sensitive to thickness (Dai et al. , 2004). If wave and wind rafting effectively increase the thickness at the expense of areal growth at the ice boundary, new ice at the edge could survive to accelerate seasonal ice cover growth. Waves and winds raft ice floes rapidly thickening the ice cover. Waves and winds also advect ice floes to create new open water for more ice production. Hopkins and Ackley (2001) suggested the existence of an equilibrium thickness of pancake ice in a wave field in the basis of numerical experimental results. They utilized a three dimensional discrete element model to simulate the movement of pancake ice in a wave field. Dai et al. (2004) utilized laboratory experiments and numerical simulations to determine the rafting process under the wave action. They proposed a theory that the equilibrium thickness is proportional to the square of both wave amplitude and floe diameter and is inversely proportional to the cube of the wavelength. This theory also provides a way to calculate the speed with which the boundary between the single-layer pancake ice floes and the equilibrium rafted ice cover propagates. Sutherland and Dumont (2018) used the ocean surface wave radiation stress to estimate the comprehensive force applied by waves in the Marginal Ice Zone. This force is balanced by an ice internal comprehensive stress based on Mohr-Coulomb granular material theory allowing the estimation of the ice thickness in the Marginal Ice Zone.

Although wind and wave rafting are evident, no much previous study relating the resulting ice cover thickness to wind and wave characteristics has been conducted. In this study we utilize experiments in a laboratory wave-wind-ice tank to understand the pancake ice rafting due to the combination of wave and wind. Pancake ice initially floats on the water surface. A persistent random wave field with JONSWAP spectrum was generated and no ice rafting was observed. The ice starts rafting as the wind is generated. Five different wind velocities were tested and the rafting process were monitored using cameras.

2 Experimental setup

Experiments were conducted at the University of Melbourne in a facility consisting of a wave flume to which a wind tunnel is attached, as shown in Fig. 1, housed inside a refrigerated chamber, where air temperatures can be reduced to $-15°$ C. The flume and wind tunnel are made out of glass supported by a wooden frame, ensuring optical access and that the structure experiences minimal contraction or expansion during freezing and defrosting. The flume is $14\,m$ long, $0.76\,m$ wide, and was filled with fresh water $0.45\,m$ deep. It is bounded at one end by a computer-controlled cylindrical wave-maker; and at the opposite end by a linear beach with slope $1:6$, which absorbs wave energy (95% energy-effective for waves tested). The wind tunnel is placed on top of the flume starting right after the wave maker and it is $12\,m$ long. Wind is blown on the water surface, it passes along the flume and is sucked from the end of the flume. Fig. 1 shows a detailed sketch of the experimental configuration. To model the pancake ice, ≈ 0.03 m thick ice cubes were placed into the water in a $2.5\,m$ long area, giving the ice area density of $\sigma_{ice} = 13.3\,kg/m^2$, starting at $6.7\,m$ from the beginning of the flume. A metallic grid was placed right after the ice-covered area, which is $9.5\,m$ from the beginning of the flume. A camera with sampling rate of $30\,Hz$ and resolution of 1920×1080 pixels was deployed at the distances $x = 8.8\,m$ from the beginning of the flume (i.e. before the metallic grid).
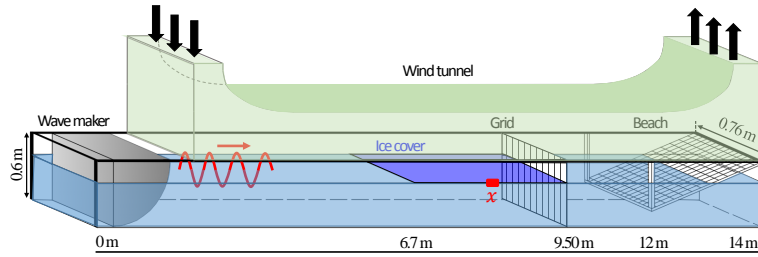

Figure 1: Schematic of the flume, with the wave maker at the left-hand end and the beach at the right-hand end. Grid is located at $x = 9.5\,m$ from the flume upstream. The light-blue is the water and the dark blue is the initial ice cover. Red rectangle indicates the camera location at $x = 8.8\,m$.

Random incident wave fields were generated from a JONSWAP spectrum as a function of the angular frequency $\omega = 2\pi f_{wave}$

$$S(\omega) = \frac{\alpha g^2}{\omega^2}\Big[-\frac{5}{4}(\frac{\omega_p}{\omega})^4\Big]\gamma^r \quad , \qquad r = \Big[-\frac{(\omega - \omega_p)}{2\sigma^2 {\omega_p}^2}\Big] \tag{1}$$

where α is the Phillip's constant, g is the gravitational acceleration, ω_p is the peak frequency, γ is the peak coefficient, and σ is the spectral width parameter. The spectra with the peak frequency of $f_{wave} = 1.25\,Hz$ and incident non-dimensional amplitude of $ka_{inc} = 0.08$ ($ka = kH_s/2$ where H_s is the significant wave height) was tested with the value of α chosen accordingly. A peak enhance coefficient $\gamma = 1$ was used. Five different time-series were generated from each JONSWAP spectrum using a Inverse Fast Fourier Transform algorithm with uniformly distributed random phases within the interval $[0, 2\pi]$ and Rayleigh distributed random amplitudes.

Five different wind speeds of $V_{wind} = 5.2, 6.7, 7.6, 9.2$ and $10.5\,m/s$ (e.g. $f_{wind} = 17, 21, 25, 29,$ and $33\,Hz$) were generated. With the ice at the desired initial condition, the wave-maker was run and wind generator was used to generate the specified fields for $5\,min$ and three repetitions for each test. After each test, the experimental configuration was reset to the initial condition in order to get ready for the next test. To measure the ice rafting, an image processing technique was used to to convert video frames from RGB into grey-scale. The air-ice-water interfaces were identified based on their luminances. Observations are accurate to 1 pixel $\approx 0.0215\,mm$.

3 Result

Fig. 2 shows consecutive snapshots of rafting over the wind speed decline from $10.5\,m/s$ to zero. The rafting thickness dramatically declines by decreasing the wind speed. The rafting gradient (rafting thickness fluctuation over the wave period) is very large for the high speed winds. Rafting gradient is approximately zero for the lowest speed wind. Results show that the rafting thickness also varies over time as the random wave amplitude

varies (see Fig. 3; where $\delta\eta$ is the instantaneous rafting thickness). For each test, the maximum rafting thicknesses occur when the maximum amplitude of the random wave approaches. Rafted ice hits the ice cubes to the metallic grid, which means that the grid undergo an extreme load. Regarding the rafting thickness distribution over distance along the flume, the thinnest rafting thickness occurs at the beginning of the ice cover (i. e. in vicinity of the open water). The maximum rafting thickness appears next to the grid. For each individual test, the mean rafting thickness over the time of $5\,min$ was calculated. Then, the rafting thickness for three repeated tests was averaged. Fig. 4 shows the average rafting thickness distribution over each wind speed. Linear and quadratic regressions are overlaid. Results show that rafting ice thickness dramatically increases by increasing the wind speed. The rafting ice thickness increasing trend is more quadratic-wise than linear-wise by increasing the wind speed.
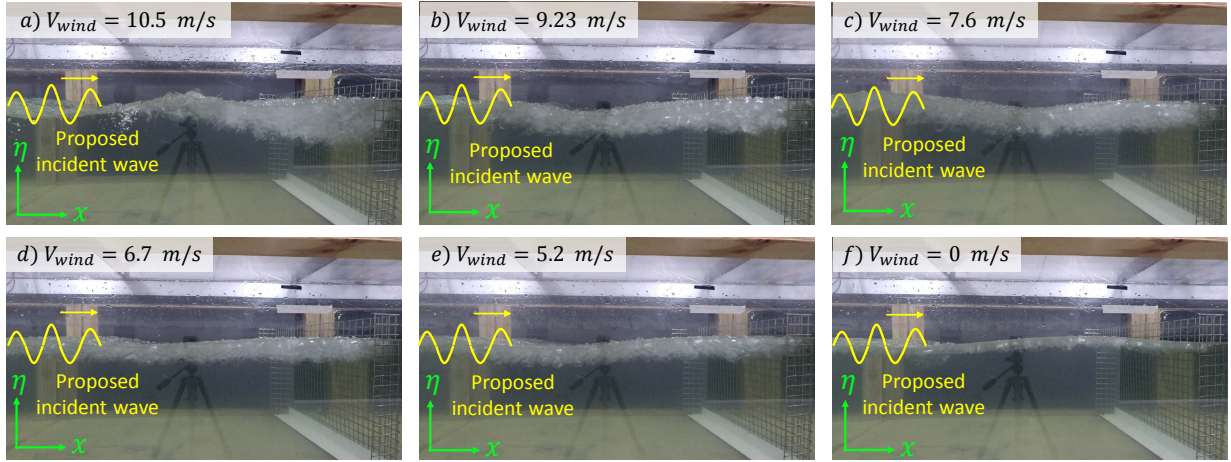

Figure 2: (a–f) Rafting thickness of various wind speeds at $x = 8.8\,m$ and $t = 150\,s$.

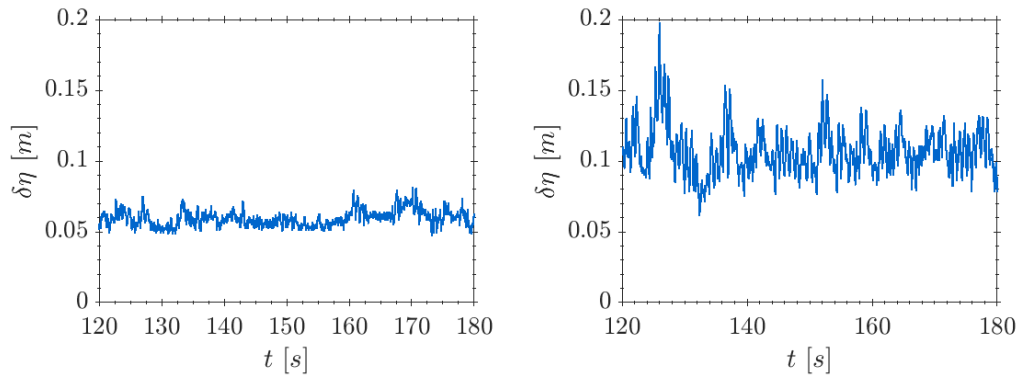Figure 3: Rafting thickness time series: $V_{wind} = 17\,m/s$ (left) and $33\,m/s$ (right), $x = 8.8\,m, t = 120 - 180\,s$.

4   Conclusion

Laboratory experiments were conducted at the University of Melbourne in a wind-wave-ice facility consisting of a wave flume housed inside a refrigerated chamber to understand the influence of wind speed on pancake ice rafting. The pancake ice initially floats on the water surface while a persistent random wave field with JONSWAP spectrum was generated. The ice starts rafting as the wind is generated. Five different wind velocities were tested and the rafting process were monitored using a camera. Results show that rafting ice thickness dramatically increases by increasing the wind speed.
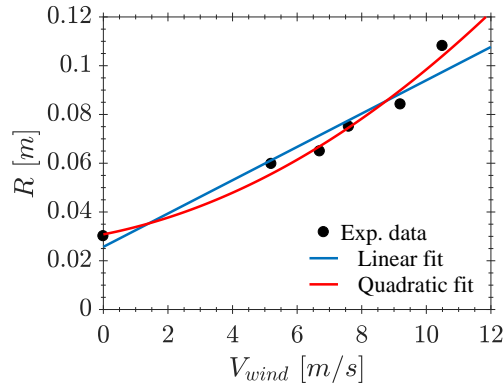
Figure 4: Rafting thickness vs wind speed. Linear (blue) and quadratic (red) regressions.

Acknowledgements

References

S. F. Ackley and H. H. Shen Pancake ice formation in a laboratory wave tank. *Eos Trans*, AGU, 77(22), 1996. West. Pac. Geophys. Meet. Suppl., 54.

T. Toyota A study on growth processes of sea ice in the southern region of the Okhotsk Sea, evaluated from heat budget and sea ice sample analysis. , 1998.

S. Martin, and P. Kauffman A field and laboratory study of wave damping by grease ice. *Journal of Glaciology*, 27(96): 283-313, 1981.

J. Bauer and S. Martin A model of grease ice growth in small leads. *Journal of Geophysical Research: Oceans*, 88(C5): 2917-2925, 1983.

L. D. Anderson Growth rate of sea ice. *Journal of Glaciology*, 3(30): 1170-1172, 1961.

W. D. Hibler III and S. F. Ackley Numerical simulation of the Weddell Sea pack ice. *Journal of Geophysical Research: Oceans*, 88(C5): 2873-2887, 1983.

M. A. Hopkins and H. H. Shen Simulation of pancake-ice dynamics in a wave field. *Annals of Glaciology*, 33: 355-360, 2001.

M. Dai, H. H. Shen, M. A. Hopkins and S. F. Ackley Wave rafting and the equilibrium pancake ice cover thickness. *Journal of Geophysical Research: Oceans*, 109(C7), 2004.

P. Sutherland and D. Dumont Marginal ice zone thickness and extent due to wave radiation stress. *Journal of Physical Oceanography*, 48(8): 1885-1901, 2018.

A. Alberello, M. Onorato, L. Bennetts, M. Vichi, C. Eayrs, K. MacHutchon and A. Toffoli Brief communication: Pancake ice floe size distribution during the winter expansion of the Antarctic marginal ice zone. *The Cryosphere*, 1-9, 2018.